Modelling and Initialization of a Virtual Synchronous Machine for Power System Fundamental Frequency Simulations

Bojana Barać, Matej Krpan, *Student Member, IEEE*, Tomislav Capuder, *Member, IEEE*, and Igor Kuzle, *Senior Member, IEEE*

Abstract—The share of renewable energy sources interfaced to the bulk power system through power electronic devices is continuously increasing. As a result, The power systems of the future face challenges of stability and reduced inertia and, to maintain the stability of the low-inertia systems, various concepts of grid-forming converter control schemes have been introduced, which enable converters to behave similarly to traditional synchronous machines. As the research in this area is gaining on importance, the sheer amount of papers with models for different kinds of simulations and the complexity of control algorithms may be daunting for newcomers in this field to understand them and to start modeling such devices. Moreover, different control schemes are often erroneously used interchangeably which adds to the confusion. This papers aims to give a clear understanding of the above aspects by explaining details of modeling and initialization of grid-forming converter control schemes for power system fundamental frequency dynamic simulations (RMS simulations) by using an example of a virtual synchronous machine (VSM). Starting from comparison of traditional systems and systems with a high share of converters and continuing with a functional overview of virtual inertia based converters in modern power systems, a step-by-step initialization of the static and dynamic model is given, focusing on RMS simulations. Finally, selected simulation examples are shown which illustrate main characteristics of virtual synchronous machines and their comparison to real synchronous machines.

Index Terms—low-inertia, grid-forming converters, virtual synchronous machine, power system, fundamental frequency simulation, power system modeling, dynamic model initialization

I. INTRODUCTION

In December 2019, the European Commission presented the European Green Deal, its flagship plan that aims to make Europe climate neutral by 2050 [1]. To satisfy the Paris Agreement of being CO_2 neutral by 2050, there is an increasing amount of renewable energy sources (RES) being integrated into power systems worldwide [2]. The most represented RES are photovoltaic (PV) panels and wind turbines [3] since they are among the most environmentally friendly and abundant [4] sources. Additionally, the level of RES integrated in the distribution network systems have been continuously growing in the last decade making power systems decentralized [5]. In 2019, a record amount of renewable energy was achieved,

accounting for over 40% of the growth in primary energy and 10% in power generation [6]: wind energy provided the largest contribution to renewables' growth (1.4 EJ) followed closely by solar (1.2 EJ). To decarbonise the power system by 2050, RES must grow even stronger [6].

Traditionally, power system operation is based on producing electrical energy from thermal and hydro power plants based on synchronous rotating machines (SM). Synchronous turbine-generators (SGs) store kinetic energy and provide rotational inertia on which the synchronized operation of the power system is based [7], [8]. In the event of a power imbalance (e.g. loss of generators, loss of loads, tie line faults, system splits, etc.) inertia helps to reduce the rate of frequency change [9], [10] allowing more time for the automatic control mechanisms and the system operator to take actions [8]. Furthermore, SGs provide voltage control by their reactive power capability. Therefore, SGs and their control mechanisms were the key in maintaining stability of the traditional power systems.

On the other hand, RES behave differently than conventional, centralized generation facilities. Most new RES are connected to the grid via power electronic converters and their power production is more complex to predict. Converter-interfaced units do not provide rotational inertia to the grid (e.g. PV units), even if physical inertia exists on the device-side of the converter (e.g. wind turbines) [7]. In case these units do not participate in provision of systems ancillary services, as is the case in most countries, displacing conventional generators with converter-connected resources can result in reduced systems capability to maintain system angle, frequency and voltage stability [9], [11]. Such systems are often referred to as low- or zero-inertia systems. In low-inertia networks the dynamics are generally faster and new interactions of dynamic phenomena arise between converter-based units and synchronous units [12] which are still being researched. Nevertheless, the technical capability to operate a low-inertia system exists which means that, if adequately implemented, the converter-based power system could be superior to the traditional one both in terms of controllability as well as in the response time to deviations and disturbances.

The challenge of operating a low-inertia system is not a challenge of tomorrow, but already of today. Although low-inertia systems are characteristic for island systems such as UK or Nordic countries, the reduction of inertia is happening in large, interconnected systems such as the continental Europe as well. Therefore, system operators of smaller, island systems

Bojana Barać, Matej Krpan, Tomislav Capuder and Igor Kuzle are with the Department of Energy and Power Systems of the University of Zagreb Faculty of electrical engineering and computing, Zagreb, Croatia (e-mail: bojana.barac@fer.hr; matej.krpan@fer.hr; tomislav.capuder@fer.hr; igor.kuzle@fer.hr).

as well as ENTSO-E have recognized the need for utilizing the advantages of converter based power plants into the ancillary service markets, such as emulated inertia, fast frequency response, voltage control, etc. [13]–[18].

From the perspective of control in AC grids, power converters can be classified as grid-feeding (i.e. grid-following), grid-supporting and grid-forming [19], and they act as interfaces between RES and the grid [20]. Nevertheless, from the electric circuitry perspective, the difference lies in whether they are modeled as a current source (grid-following) or as a voltage source (grid-forming). In both cases, grid-supporting means that they provide ancillary services by modifying their setpoints based on local measurements [21], although some research suggests the distinction is even more subtle and depends on the implemented control algorithm [22]. Today's converter-interfaced resources that are connected to the bulk power system are typically grid-following in order to precisely regulate the active and reactive power exchanged with the network. On the downside, they must be synchronized with the grid voltage of the point of common coupling (usually via a phase-locked loop), cannot operate in island mode (at least one synchronous generator or a grid-forming converter is necessary) and have trouble operating in weak grids. To tackle this issue, the concept of *Virtual Synchronous Machine* (VSM) has been introduced in the literature. It is designed to mimic the basic dynamic behavior of a classical synchronous turbine-generator, which is providing inertia, damping, primary frequency control, voltage control and capability to operate off-grid.

There are different implementations of the VSM in the literature and they are often mistakenly perceived as identical. High-fidelity models are usually found in the literature that include either semiconductor switching phenomena or averaged models in the electromagnetic transient (EMT) time domain. What the existing literature is missing is a comprehensive overview of VSM implementation and simulation in commercial power system simulation software, which often has limited or less flexible dynamic simulation environment compared to e.g. Simulink. This paper aims to demystify and clarify different VSM implementations and provide a comprehensive step-by-step guide on how to implement it in commercial power system simulation software starting from steady-state model (load flow), through dynamic framework with defined inputs and outputs to the initialization of the dynamic model, and finally RMS simulations which are still the key in performing dynamic simulations of bulk power systems.

The paper is envisioned as a tutorial to assist the early-career researchers, students, practical engineers in the industry as well as others and contributes by:

1) Providing a review and technical explanation of the different grid-forming converter control schemes that emulate the behavior of a synchronous machine, with a goal to demystify their subtle differences and to show how to implement a detailed dynamic model with a straightforward initialization procedure. The later is given as a step-by-step guidance emphasizing the key aspects and pointing out the usual pitfalls.

2) Enabling open source/access model presented in the paper as a backbone for future research and development of the above mentioned target groups.

The prerequisite background of the reader, required to understand and follow this paper, is the basic understanding of power system analysis (load flow), power system dynamic operation and modeling of systems of differential equations.

The rest of the paper is organized as follows: Section II gives an overview of the different implementations of VI-based converters. In Section III a static model, system layout and values of used parameters are explained to execute load flow analysis. The dynamic models are presented in Section IV. Initialization of the model is given in Section V. Finally, selected simulation examples are provided in Section VI.

II. IMPLEMENTATIONS OF THE VIRTUAL SYNCHRONOUS MACHINE

Virtual inertia (VI)-based converters solve the problems introduced by converter-connected sources. In literature, VI-based converters can be found under different names, such as: virtual synchronous machine (VSM), *virtual synchronous generator* (VSG), *synchronverter*, etc. Each concept arose from the structure and mathematical model of the SM [23]. SM includes synchronous generators and synchronous motors. All the control methods present an idea of operating a converter like a synchronous machine, however there are minor differences between each of them [24]. A general mathematical model of all VI-based converters is based on emulating the swing equation (1) of a SM [20]:

$$P_{\text{gen}} - P_{\text{load}} = J\omega_r \frac{d\omega_r}{dt} \tag{1}$$

where P_{gen} is the generated power, P_{load} is the power demand with losses, J is the total machine inertia, and ω_r is the rotor speed. The above equation shows that the relation between the SM rotor speed (system frequency) is proportional to the imbalance between generation and load. The VI-based converters allow RES to participate in frequency regulation by controlling their output power during frequency disturbances. The ability to choose and change the parameters during operation (e.g. inertia, field inductance, mutual inductance and friction coefficient) shows a great advantage over actual SGs. Unlike real SMs, these parameters are not defined by the actual construction of the machine; rather, they can be completely arbitrary since they are just a part of the control software. Three most common topologies of the VI-based converters are shown in Fig. 1, in which the gray blocks and black lines are common for all implementations.

A. VSM

The VSM is a grid-forming control scheme which emulates the static and dynamic performance of a SG. General structure of the VSM is shown in Fig. 1 by gray and blue elements. Its virtual inertia topology is based on the swing equation with

Figure 1: VI-based converters: Synchronverter, VSG and VSM

frequency droop control (2), written in per-unit (p.u.) in this case.

$$\frac{d\omega_{VSM}}{dt} = \frac{1}{T_a}\bigg(p^* + k_\omega \left(\omega_{VSM}^* - \omega_{VSM}\right) - p \tag{2}$$

$$- k_d \left(\omega_{VSM} - \tilde{\omega}_g\right)\bigg)$$

where ω_{VSM} and ω^*_{VSM} are the speed of the virtual rotor and speed reference in p.u., respectively; T_a is the virtual mechanical time constant equivalent to $2H$ in a traditional SM in seconds; p^* is the external power reference in p.u.; p is the measured output electrical power in p.u.; k_ω is the droop gain of the virtual governor, k_d is the damping constant and $\tilde{\omega}_g$ is the measured grid frequency in per-unit. In a real SM damping torque depends on the operating point of the machine. A model with constant k_d will not mimic the SM behavior throughout the entire operating range [25]. Referring to Fig. 1, the output of the reactive power control is the voltage amplitude reference while the outputs of the active power control block, which includes the swing equation, are the frequency and phase angle references. These references serve as inputs for the cascaded voltage and current control [26]. An application of the cascade loop ensures controllability and flexibility for protection strategies, because limitations of the voltages and currents of the converter are included [25].

The phase-locked loop (PLL) estimates the actual grid frequency by measuring the grid voltage and is used only for the implementation of the damping effect in (2). It is not needed for the synchronization, nor the current or voltage control rely on it as in conventional, grid-following VSC [26]. A virtual impedance is included in the VSM to facilitate power-frequency droop control in resistive grids [27]. Since it is based on the mathematical model of a SG, the VSM is modeled in a rotating direct-quadrature (*dq*) reference frame (in this case, in the synchronous reference frame) [26].

The first model was introduced in 2007 in [28] and named VIrtual Synchronous MAchine (VISMA). Unlike the VSM described above, VISMA is considered as a current source and

cannot operate in island mode. In [29] a three-phase model of VISMA is presented. Compared to a *dq* model, a three-phase model of VISMA is more operative under asymmetrical load conditions or during rapid disturbances in the grid [29]. There is also the Institute of Electrical Power Engineering (IEPE's) topology that represents the VISMA operating as a voltage source which offers better performance in islanded mode, however in the grid-connected mode it exhibits some issues during grid synchronization due to transient currents [30].

Another approach is the virtual synchronous machine with zero inertia constant H (VSM0H) [31], [32]. VSM0H has no PLL and no inner current loop. Active and reactive power control loops generate the voltage amplitude and frequency based on reactive power – voltage and active power – frequency droops, as shown by (3) and (4).

$$f^{**} = f^* + D_f(p^* - p)\left(1 + \frac{k_d s}{1 + \tau_{kD} s}\right) \tag{3}$$

$$\mid E \mid = v^* + D_v(q^* - q) \tag{4}$$

The active and reactive power measurements are filtered using boxcar filters which remove higher harmonics during unbalanced or distorted grid conditions while ensuring steady values of frequency and voltage amplitude. However, a PMU-class frequency measurement is needed for the filtering. Because there is no "inertia", this control strategy does not reduce the RoCoF right after the event, although the nadir is well-managed. Significant frequency deviations can cause large changes in output power.

Finally, an advanced version of VSM is the Self-Tuning VSM (ST-VSM) which varies the damping coefficient and virtual inertia constant during operation using online optimization algorithms [33].

B. VSG

Generally speaking, VSG can be considered to fall under Swing-Equation Based Inertial Response (SEBIR) methods which add the swing equation to *dq*-axis controllers

with current injection (DQCI) [31]. General structure of the VSG/SEBIR converter is shown in Fig. 1 by gray and red elements.

After a power imbalance in the system, SEBIR will detect the RoCoF and add the signal ΔP proportional to RoCoF active power reference. The virtual inertia results using SEBIR were not promising [32], because the response time of SEBIR is slower than inertial response of conventional SMs [34]. SEBIR converters require a PLL for synchronization, regardless of the way the grid frequency is estimated for inertial response. This type of control is also well-known under virtual or synthetic inertia control.

The swing equation for inertia emulation of the VSM (2) can be reformulated to extract the power reference expression (5). It is assumed that the electrical power p is controlled by converter. The VSM reference frequency is replaced by the grid reference frequency ω_g^* and the VSM rotor frequency ω_{VSM} is replaced by the measured grid frequency $\tilde{\omega}_g$ [25].

$$p^{**} = p^* + k_\omega(\omega_g^* - \tilde{\omega}_g) + k_i \frac{d\tilde{\omega}_g}{dt} \qquad (5)$$

k_ω is the steady state droop gain and k_i the inertia constant [25]. Depending on the sign of the $\frac{d\tilde{\omega}_g}{dt}$, the VSG will absorb or inject power.

With this approach, the internal model of the machine inertia is not established and an external voltage and physical inertia must exist [25]. Consequently, the VSG can not operate in islanded mode. The output of the reactive power control is the reactive power reference q^{**}, and the output of the active power control is the active power reference p^{**} [23], [25], as shown in Fig. 1. Current references are calculated based on p^{**} and q^{**}, and the measured grid voltage at the point of common coupling $\tilde{v}$. The term VSG has been coined around 2008 [35] based on some earlier research in this area, but it does not imply the capability of standalone operation, unlike a real SG.

C. Synchronverter

General structure of the synchronverter machine is shown in Fig. 1 by gray and green elements. Synchronverter's topology is based on a synchronous generator model. The synchronverter can be illustrated like a SG with a small capacitor bank connected in parallel to the stator [23], [36]. In dynamic equations of SG, the mechanical power exchanged with the prime mover is replaced with the power exchanged with the DC bus. The synchronverter consists of a conventional converter, filter inductors, capacitors and controller. A synchronverter has all advantages and disadvantages (e.g. oscillations around the synchronous frequency) of a SG. The synchronverter can be operated like a synchronous motor. The concept of the synchronverter is similar to the VSM, but with simpler control logic. The initial model of the synchronverter required a PLL for grid synchronization, but once synchronized, the PLL is not needed anymore. Unlike the VSM, the voltage amplitude reference and phase angle are directly used to drive the gate signals [25], as shown in Fig. 1. Therefore, this implementation does not have the cascaded voltage-current control loops. Consequently, the constraints of the converter

cannot be included in this structure and the protection is harder to implement [25]. An advanced model is self-synchronizing without the PLL requirement. It is substituted with an active power synchronization loop with virtual impedance.

D. Summary

Although in literature (e.g. [37]) these three control strategies (VSM, VSG/SEBIR and synchronverter) are often perceived as identical, subtle differences have been shown and explained. Even though historically the VSG implies grid-following current source behavior, we argue it is much more intuitive to equalize the terms VSM and VSG to imply grid-forming voltage source behavior since all synchronous generators can operate without the presence of an external grid. Thus, the differentiation between VSMs and grid-following units with virtual/synthetic inertia enabled (SEBIR) would be clearer and more intuitive. VSM taxonomy is given in Table I.

There are others approaches of VI-based converters, such as: inducverters that behave as induction generators; a VI-based static synchronous compensator which mimics synchronous condenser and virtual oscillator controller (VOC) that enables synchronization of RES without dedicated communication [30]. Their implementations are out of the scope of this paper.

III. STEADY-STATE REPRESENTATION

In this paper, the modeling and simulations are done in DIgSILENT PowerFactory, however the presented procedure is equivalent for any other commercial power system simulation software. The shown VSM model is used to control a static self-commutated switching power converter supplied from an electric energy source.

The first step is to create a 1-port network element which represents a converter-based source and is interfaced to the power system model via a VSC (e.g. a *static generator* element in PowerFactory, a *disperse generation* element in NEPLAN, etc.). The static generator is connected to the grid through an three-phase LC filter to attenuate higher harmonics due to switching. However, this functionality will not be visible in RMS simulations since it assumes only the fundamental frequency component and no higher harmonics. Nevertheless, LC filter will impact reactive power flow. The presented VSM model can be implemented without the LC filter for RMS simulations, but this is beyond the scope of this paper.

To enable the grid-forming behavior, the static generator must necessarily be considered as a voltage source, not current source by setting the appropriate parameter in the network element. For load-flow analysis, the static generator can operate in PQ (operating with defined active and reactive power injections), PV (operating with defined active power injection and controlling the terminal voltage magnitude) or as a swing bus if this element is a reference machine in the power system model (defining the voltage magnitude and angle of the respective bus). For a simple single-machine infinite bus system shown in Fig. 2 (single-phase equivalent circuit) the static generator is set as the reference machine

Table I: Taxonomy of VSM implementations

Reference	Control strategy	Strenghts	Weakness
[28]	VISMA	- fast current control - application in microgrids - direct limitations of current reference	- high frequency noise due to converter's switch activity - numerical instability
[38], [39]	VSG	- emulation of dynamic performance of SG - ability of absorbing or injecting power in the grid - fast response in tracking steady-state frequency - inherent overcurrent protection	- inability to operate in islanded mode - an internal model of the machine inertia is not established - instability due to PLL
[36]	Synchronverter	- ability to operate as SG and motor - possibility to choose the parameters that are impossible in convencional SG - only earlier versions required PLL - models without PLL are cheaper, easier in tuning and have lower computional time	- no inherent protection - protection is hard to implement - constrains of the converter are not included
[26], [27]	VSM	- fast frequency response - emulation of static and dynamic performance of SG - power-sharing ability - automatic synchronization - ability of islanded operation - controllable and flexible protection strategies - PLL used only for synchronization	- complex PLL implementation - limited flexibility during tranzient conditions due to fixed parameters - SG behaviour in the entire operating range is not covered
[34]	SEBIR	- no PLL - use of symmetric filters for frequency measurement	- slow response time - complicated algorithms and expensive communication network required
[31], [32]	VSM0H	- no PLL - steady measured values during unbalanced scenarios - leads to a system with zero inertia in the future	- the RoCoF is not reduced right after the event - requires a boxcar filters for measurement - expensive communication network required - algorithms are computationally heavy
[33]	ST-VSM	- adapting the values of virtual inertia and damping coefficient - efficient control during tranzient conditions - use of online optimization algorithms to find optimal parameters - emulation of SG behaviour in the entire operating range	- a greater discharge of ESS than VSM with fixed parameters - sufficient processing power should be provided - high computational burden

in islanded mode, while in grid-connected mode the external grid is set as the reference. This is important so that the reference frame transformations are done correctly; note that the reference machine defines the global (grid) synchronous rotating reference frame.
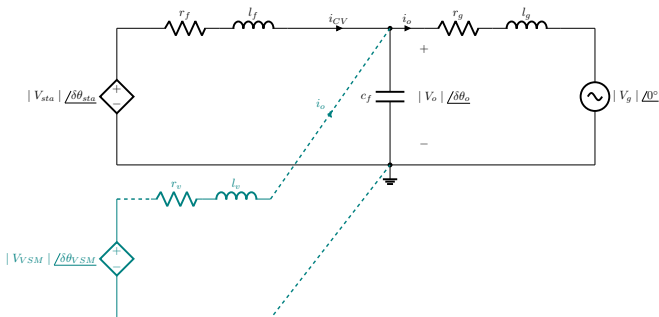

Figure 2: Single-phase equivalent circuit of the static generator connected to the grid

In Fig. 2, the components that physically exist are shown in black. The external grid is represented by a voltage source with the corresponding internal impedance which can also include coupling impedance of lines and transformers. The dashed teal part shows the equivalent virtual circuit of the VSM and it has no physical meaning. Analogous to the equivalent circuit of a SG, the controlled current i_o causes a virtual voltage drop across the virtual impedance $r_v + j\omega_{VSM}l_v$. The virtual internal voltage vector $\boldsymbol{v}_{VSM}$ is obtained by summing the voltage vector measured at the point of common coupling $\boldsymbol{v}_o$ and the voltage drop across the virtual impedance. Hence, $\boldsymbol{v}_{VSM} = \mid V_{VSM} \mid \underline{/\delta\theta_{VSM}}$ would be the equivalent of the internal electromotive force (EMF) of a SG. The relation between voltage vectors is shown in Fig. 3.

The modeling and control of the electrical system is implemented in the synchronous rotating reference frame. The global reference frame is aligned with the reference machine voltage vector and it rotates with the speed of the reference
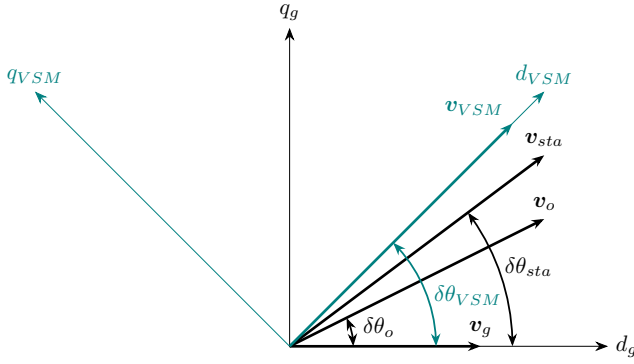
Figure 3: Vector diagram

machine, in this case with the external grid v_g. All other voltage vectors are phase displaced relative to the phase of the reference machine. Therefore, the measured values have to be transformed to the VSM-oriented dq frame to be used in the VSM control strategy. For example, the voltage v_o is measured at the point of the common coupling and it leads the grid voltage vector by the phase angle $\delta\theta_o$. To transform it to the VSM-oriented reference frame, expression (6) is used:

$$v_o^{VSM} = \mid v_o \mid e^{j(\delta\theta_o - \delta\theta_{VSM})}. \tag{6}$$

IV. DYNAMIC MODEL

Fig. 4 shows the VSM model from [26] implemented in this paper with all the necessary blocks and signals to implement it in commercial power system simulation software. Each component can be described by equations or block diagrams. A general control strategy of VSM consists of: voltage and reactive power control, virtual inertia and active power control, virtual impedance, voltage control, active damping, current control and phase-locked loop (optionally for implementation of the damping term; not needed for the synchronization or control).

A. Reference frame transformations

The measurement devices in the simulation packages (e.g. PowerFactory) usually output the real and imaginary components of the measured values in the global SRF aligned with the reference machine. The variables in the global reference frame are labeled with "r" (real) and "i" (imaginary) indices. The variables used as input signals for the VSM model must be transformed to the local VSM-oriented reference frame (labeled with "d" and "q" indices) by (7). This is what the *ri/dq transformation* block does.

$$v_o^{VSM} = (v_{r,o} + jv_{i,o}) \cdot e^{-j\delta\theta_{VSM}} \tag{7}$$

The d- and q-components are given by (8) and (9):

$$v_{d,o} = v_{r,o}\cos(\delta\theta_{VSM}) + v_{i,o}\sin(\delta\theta_{VSM}) \tag{8}$$

$$v_{q,o} = v_{i,o}\cos(\delta\theta_{VSM}) - v_{r,o}\sin(\delta\theta_{VSM}) \tag{9}$$

The currents are transformed analogously using the same rotation by $e^{-j\delta\theta_{VSM}}$. The voltage v_o is measured at the point

of the common coupling, i.e. at the capacitor (Fig. 2). The direction of the currents i_o and i_{CV} is shown in Fig. 2.

Note that special attention must be paid to the connection of the measuring elements so that the signs of the measured values are correct and consistent throughout the model. Otherwise, the model may become numerically unstable. This is especially relevant for measuring various current signals from the grid model since the measuring element may return either positive or negative values of the same current depending on the location of measurement connection and the orientation of the measuring element. For example, the dynamic model may want to generate positive inner current references for power flowing out of the machine, while the measuring element may return negative currents for the same direction of power, thus the control system may become unstable and not numerically converge.

Likewise, control signals for the static generator have to be transformed from the VSM frame back to the global frame using the inverse transformation (rotation by $e^{j\delta\theta_{VSM}}$). This is what the *dq/ri transformation* block does (explained in more detail in section IV-H).

B. Virtual Inertia and Active Power Control

The implementation of this block is based on virtual swing-equation (10) that introduces virtual inertia and damping effect of the SG.

$$\frac{d\omega_{VSM}}{dt} = \frac{1}{T_a}\left(p^* - p - k_d(\omega_{VSM} - \omega_{PLL})\right. \\ \left. - k_\omega(\omega_{VSM} - \omega_{VSM}^*)\right) \tag{10}$$

p^* is external power reference and p is the output electric power measured after the LC filter (11). The damping effect is achieved by the damping constant k_d and comparing the VSM angular speed ω_{VSM} to the estimated grid frequency ω_{PLL}. The power-frequency droop is defined by the droop gain k_ω and difference between the VSM angular speed and its reference value ω_{VSM}^*.

$$p = v_{d,o} \cdot i_{d,o} + v_{q,o} \cdot i_{q,o} \tag{11}$$

The solution of the equation (10) gives the VSM angular speed ω_{VSM}. To determine the VSM phase displacement, it is necessary to define the speed deviation $\delta\omega_{VSM}$ (12):

$$\delta\omega_{VSM} = \omega_{VSM} - \omega_g \tag{12}$$

where ω_g is the per-unit speed signal of the reference machine which defines the global reference frame speed. Note that this signal does not exist in reality and it is only needed to properly execute the RMS simulation and define the relative position of the VSM to the reference machine. In reality, this signal would have to be estimated by a PLL, PMU, etc. The VSM phase displacement $\delta\theta_{VSM}$ is defined by (13):

$$\frac{d\delta\theta_{VSM}}{dt} = \delta\omega_{VSM} \cdot \omega_b \tag{13}$$

where $\omega_b = 2\pi f_b$ is the rated (base) angular grid frequency, equal to 100π for a 50 Hz system. This phase angle is used to create the VSM-oriented reference frame.
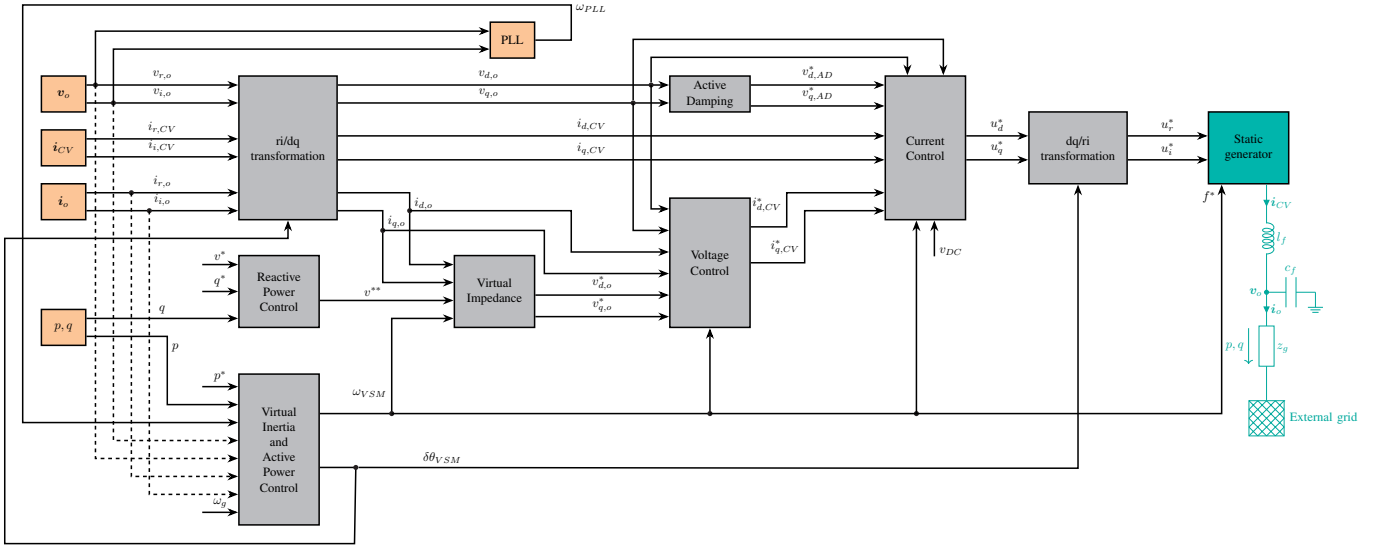
Figure 4: Control scheme of the VSM: measurement elements are highlighted in orange, user-defined dynamic model elements are in gray and network elements are in green. Dashed lines are necessary signals for initialization only.

Output ω_{VSM} is connected to the f^* input of the static generator model. This connection is only active if the static generator element is set as the reference machine in the system or a swing node, thus $f^* := \omega_{VSM}$. This is necessary because it defines the speed of the global reference frame as well as the grid frequency if the converter operates in island mode.

C. Phase Locked Loop

The PLL is used to estimate the actual grid frequency. The input signal is the voltage $\boldsymbol{v}_o$ in the grid reference frame (14). Unlike the article [26] where both d- and q-components of the voltage are estimated, this implementation transforms the positive-sequence voltage $\boldsymbol{v}_o$ in the grid reference frame to the PLL reference frame by zeroing out the d-component of the voltage in the steady-state. The q-component is then:

$$v_{q,o}^{PLL} = v_{i,o} \cos(\delta\theta_{PLL}) - v_{r,o} \sin(\delta\theta_{PLL}) \quad (14)$$

The first order low-pass filter is then used on the q-voltage component, where ω_{LP} is the cut-off frequency (15). The filtered signal $\hat{v}_{q,o}^{PLL}$ is the input signal for the PI regulator estimating the grid frequency deviation $\delta\omega_{PLL}$ (16).

$$\frac{d\hat{v}_{q,o}^{PLL}}{dt} = -\omega_{LP} \cdot \hat{v}_{q,o}^{PLL} + \omega_{LP} \cdot v_{q,o}^{PLL} \quad (15)$$

$$\frac{d\delta\omega_{PLL}}{dt} = k_{p,PLL} \cdot \frac{d\hat{v}_{q,o}^{PLL}}{dt} + k_{i,PLL} \cdot \hat{v}_{q,o}^{PLL} \quad (16)$$

The angular speed displacement is used to define the phase displacement (17):

$$\frac{d\delta\theta_{PLL}}{dt} = \delta\omega_{PLL} \cdot \omega_b \quad (17)$$

The actual grid frequency estimated by PLL is given by expression (18):

$$\omega_{PLL} = \delta\omega_{PLL} + \omega_g. \quad (18)$$

D. Reactive Power Control

The reactive power controller provides the voltage amplitude reference v^{**}. The measured reactive power q is first filtered (19) and then used to calculate the voltage reference (20).

$$\frac{d\hat{q}}{dt} = -\omega_f \cdot \hat{q} + \omega_f \cdot q \quad (19)$$

$$v^{**} = v^* + k_q(q^* - \hat{q}) \quad (20)$$

ω_f is cut-off frequency of the low-pass filter, $\hat{q}$ is filtered value of the reactive power, v^* is the external voltage amplitude reference, q^* is the reactive power reference and k_q is the reactive power droop gain. The reactive power can be expressed in scalar form in the VSM reference frame as:

$$q = -v_{d,o} \cdot i_{q,o} + v_{q,o} \cdot i_{d,o} \quad (21)$$

With the reactive power controller, the voltage droop control of the traditional SG is achieved. However, note that the VSM control structure directly controls the magnitude of the internal virtual EMF of the converter, while controlling some remote terminal in the grid is not possible in this implementation.

E. Virtual Impedance

The voltage amplitude reference is passed through a virtual impedance before it is used as an input signal to the cascaded voltage and current control. Virtual impedance has equivalent impact to the VSM phase angle as the synchronous impedance of the SG. The output signals of this block are d- and q-reference voltage components given by expressions (22) and (23):

$$v_{d,o}^* = v^{**} - r_v \cdot i_{d,o} + \omega_{VSM} \cdot l_v \cdot i_{q,o} \quad (22)$$

$$v_{q,o}^* = 0 - r_v \cdot i_{q,o} - \omega_{VSM} \cdot l_v \cdot i_{d,o} \quad (23)$$

where r_v and l_v are virtual resistance and inductance shown in teal color in Fig. 2. The virtual impedance determines the sensitivity of the VSM model to the changes in grid conditions.

Lower magnitude of virtual impedance increases the model sensitivity. Virtual impedance is necessary in power networks in which the resistances are on the same order of magnitude as inductances (e.g. MV/LV networks) in order to achieve decoupled control of active and reactive power.

F. Voltage Control

The voltage controller provides the current references for the inner current controller. The d- and q-axis voltages are compared to their references and then passed through PI controllers producing the current references i^*_{CV}. The d- and q-components of the current references are given by expressions (24) and (26):

$$i^*_{d,CV} = k_{pv}(v^*_{d,o} - v_{d,o}) + k_{iv}\epsilon_1 - c_f \cdot \omega_{VSM} \cdot v_{q,o} + k_{ffi} \cdot i_{d,o}$$
(24)

$$\frac{d\epsilon_1}{dt} = v^*_{d,o} - v_{d,o}$$
(25)

$$i^*_{q,CV} = k_{pv}(v^*_{q,o} - v_{q,o}) + k_{iv}\epsilon_2 + c_f \cdot \omega_{VSM} \cdot v_{d,o} + k_{ffi} \cdot i_{q,o}$$
(26)

$$\frac{d\epsilon_2}{dt} = v^*_{q,o} - v_{q,o}$$
(27)

where k_{pv} and k_{iv} are the PI controller gains, c_f is per unit value of the filter capacitance and k_{ffi} is the feed-forward gain that can be set to either 0 or 1 enabling or disabling the feed-forward of measured currents flowing into the grid. ϵ_1 and ϵ_2 are integrator states of the PI voltage controllers.

G. Active Damping

The block of the active damping is used to attenuate oscillations of the filter capacitor voltage $\boldsymbol{v}_o$ using a high-pass filter (28). The resulting filtered values are given by expressions (29):

$$\frac{d\phi}{dt} = -\phi \cdot \omega_{AD} + v_0 \cdot \omega_{AD}$$
(28)

$$\boldsymbol{v}^*_{AD} = k_{AD}(v_0 - \phi)$$
(29)

where ϕ represents the state of the filter with cut-off frequency ω_{AD}. These equations are used for both d- and q-components. The VSM model can operate without active damping, but in this case the transients will be more pronounced.

H. Current Control

The current controller provides the voltage reference for the static generator. Firstly, the measured converter currents and the current references are compared. Then, their difference is passed through a PI controller generating the voltage reference for the static generator. The d- and q-components of the output signals are given by expressions (30) and (32):

$$v^*_{d,CV} = k_{pc}(i^*_{d,CV} - i_{d,CV})$$
$$+ k_{ic}\gamma_1 - l_f \cdot \omega_{VSM} \cdot i_{q,CV} + k_{ffv} \cdot v_{d,o} - v^*_{d,AD}$$
(30)

$$\frac{d\gamma_1}{dt} = i^*_{d,CV} - i_{d,CV}$$
(31)

$$v^*_{q,CV} = k_{pc}(i^*_{q,CV} - i_{q,CV})$$
$$+ k_{ic}\gamma_2 + l_f \cdot \omega_{VSM} \cdot i_{d,CV} + k_{ffv} \cdot v_{q,o} - v^*_{q,AD}$$
(32)

$$\frac{d\gamma_2}{dt} = i^*_{q,CV} - i_{q,CV}$$
(33)

where k_{pc} and k_{ic} are the PI controller gain, l_f is per-unit value of the filter inductance and k_{ffv} is the feed-forward gain. γ_1 and γ_2 are integrator states of the PI voltage controllers. The resulting voltage references are then divided by the measured DC-link voltage to generate the modulation signals used to control the static generator. Modulation signals are generally in the range $[0, 1]$ to avoid overmodulation issues. In this case the DC link voltage v_{DC} is considered stiff and equal 1 p.u. because the source connected to the DC side of the converter and the respective DC voltage dynamics are beyond the scope of this paper. The input signals of the converter (static generator) are defined by (34):

$$u^*_d = \frac{v^*_{d,CV}}{v_{DC}}, u^*_q = \frac{v^*_{q,CV}}{v_{DC}}$$
(34)

Before the signals are sent to the converter, they must be transformed back to the grid (global) reference frame by rotating the *dq* space vector by $e^{j\delta\theta_{VSM}}$, described by (35) and (36):

$$u^*_r = u^*_d \cos(\delta\theta_{VSM}) - u^*_q \sin(\delta\theta_{VSM})$$
(35)

$$u^*_i = u^*_d \sin(\delta\theta_{VSM}) + u^*_q \cos(\delta\theta_{VSM})$$
(36)

Notice that the voltage and current controllers are presented with the *cross-coupling* between the d- and q-components to improve tracking. Cross-coupling is not needed and it has no effect in the steady-state, however transient behavior is improved with cross-coupling.

V. INITIALIZATION OF THE DYNAMIC MODEL

The model initialization starts with the grid elements and load flow calculation that provide the static generator modulation signals u^*_r and u^*_i.

The initialization of the dynamic model is usually performed output-to-input. The output signals of the network elements are usually known from the steady-state load flow calculation and they are used to initialize the inputs by backtracking through the model. Then, all states variables and all unknown input or output signals must be initialized. The general rule is to set all derivatives to zero ($\frac{dx}{dt} = 0$ or $s = 0$, i.e. the steady-state is observed) and solve the system of (non)linear equations.

However, with a model this complex there are two issues with the general procedure described above. Firstly, commercial power system simulation software usually has less flexible and inferior interface for dynamic modeling and initialization compared to e.g. MATLAB/Simulink. Therefore, instead of solving a complete set of equations at once, which sometimes the software will not allow or will fail at, it is better to initialize the model in a modular manner i.e. by doing it for each block separately which is also easier to debug. Secondly, such a model cannot be sequentially initialized output-to-input since there are not enough data known starting from the output of

the dynamic model (which are modulation signal inputs to the static generator element). Some data from the dynamic model input is also known and the whole model must be simultaneously initialized input-to-output and output-to-input while solving the conflicts when the two sides meet. Therefore, this paper presents a modular, straightforward initialization procedure.

The initialization flowchart is summarized in Fig. 5. The process is described in more details in the following subsections. The integration step size of the RMS simulation should be set to 1 ms with 10 ms maximum step, otherwise oscillations due to numerical stability issues will arise.

A. Initialization from input to output

PLL input signals are known and the outputs need to be initialized. In the steady-state the angular speed deviation is zero and the actual grid frequency corresponds to the rated value (37). The phase displacement is initialized using positive-sequence voltage components calculated by load flow. It is equal to the phase angle of the measured voltage (38) relative to the reference machine.

$$\omega_{PLL} = \omega_g^* \tag{37}$$

$$\delta\theta_{PLL} = \tan^{-1}\left(\frac{v_{i,o}}{v_{r,o}}\right) \tag{38}$$

In steady-state the VSM angular speed deviation is zero and the VSM frequency is equal to ω_g^*. To initialize the VSM phase displacement, voltage at the point of common coupling $\boldsymbol{v}_o$ and the current flowing to the external grid $\boldsymbol{i}_o$ must be measured. According to Fig. 2 the current $\boldsymbol{i}_o$ causes the voltage drop across the virtual impedance. Consequently, the VSM internal voltage vector is defined by (39):

$$\boldsymbol{v}_{VSM} = \boldsymbol{v}_o + \boldsymbol{i}_o \cdot (r_v + jx_v) \tag{39}$$

Note that the $\boldsymbol{v}_o$, $\boldsymbol{i}_o$ are left in the global reference frame since the internal load angle of the VSM is defined as relative to the reference machine. The steady-state value of the VSM phase displacement is defined by real and imaginary components of the VSM voltage (40):

$$\delta\theta_{VSM} = \tan^{-1}\left(\frac{\Im\{\boldsymbol{v}_{VSM}\}}{\Re\{\boldsymbol{v}_{VSM}\}}\right) \tag{40}$$

The external power reference p^* is equal to the measured power p in steady-state.

Observing the equations (28) and (29), it can be noticed that the filtered values will be equal to the voltage $\boldsymbol{v}_o$. Therefore, the output signals of the active damping in the steady-state are zero (41) meaning that there are no voltage oscillations. However, input to the active damping block is $\boldsymbol{v}_o$, which must be transformed to the VSM-oriented reference frame during initialization.
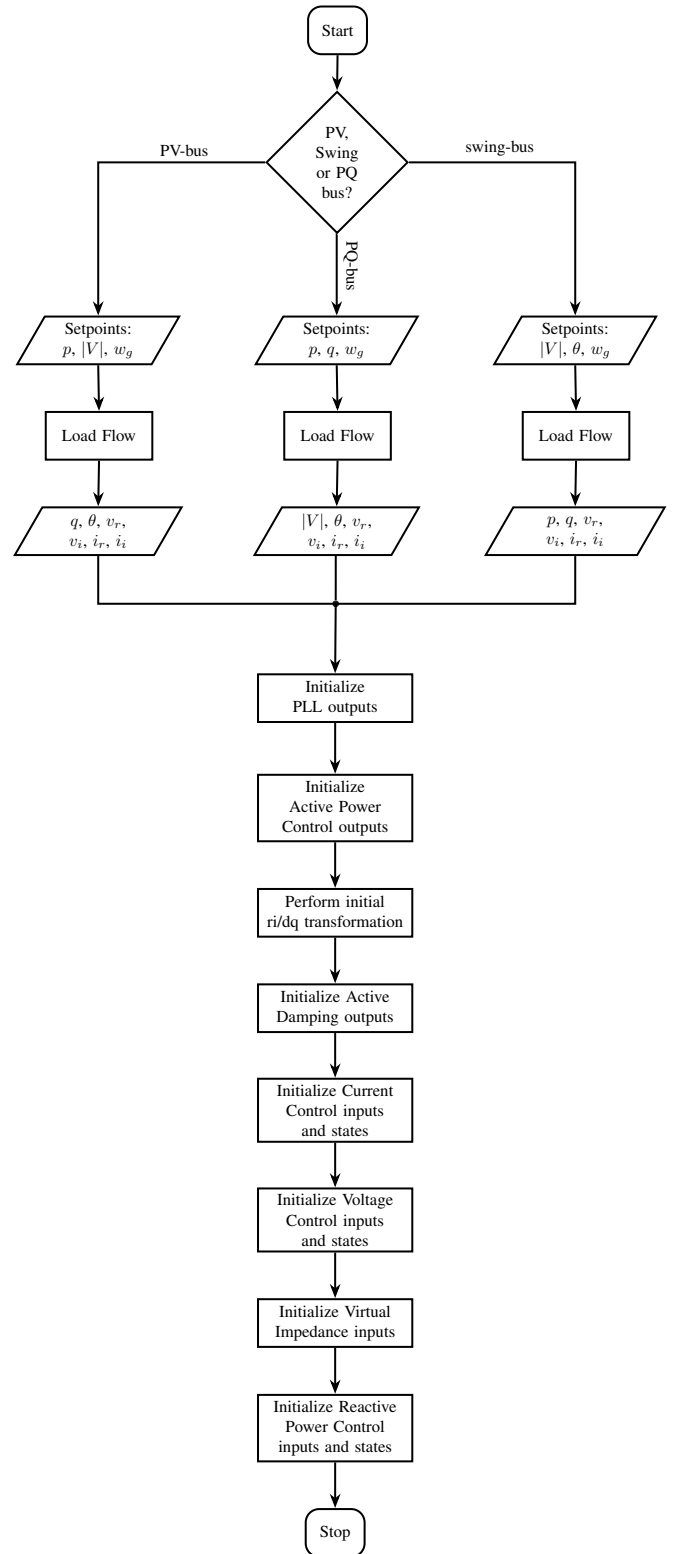
$$\boldsymbol{v}_{AD}^* = 0 \tag{41}$$

Figure 5: Initialization process flowchart

B. Initialization from output to input

The previously described initialization involved the known input signals and unknown outputs that needed to be initialized. The initialization of the voltage and current controllers is performed output-to-input. The converter control signals are

known from load flow calculation and used backwards through the current/voltage controllers, virtual impedance and reactive power controller, initializing all of them.

The converter signals u_r^* and u_i^* are measured in the grid reference frame. Hence, they are first transformed to the VSM-oriented reference frame by (42) and (43). $\boldsymbol{v}_o$, $\boldsymbol{i}_o$ and $\boldsymbol{i}_{CV}$ also have to be transformed to the VSM-oriented reference frame after $\delta\theta_{VSM}$ was initialized by (40).

$$u_d^* = u_r^* \cdot \cos\delta\theta_{VSM} + u_i^* \cdot \sin\delta\theta_{VSM} \tag{42}$$

$$u_q^* = u_i^* \cdot \cos\delta\theta_{VSM} - u_r^* \cdot \sin\delta\theta_{VSM} \tag{43}$$

Then, the converter voltage references are given by (44) and (45):

$$v_{d,CV}^* = u_d^* \cdot v_{DC} \tag{44}$$

$$v_{q,CV}^* = u_q^* \cdot v_{DC} \tag{45}$$

In steady-state the current references, that are input signals to this block, are equal to the measured currents $\boldsymbol{i}_{CV}$. Therefore, there is no control error before the PI controllers and the state variables are initialized based on the known outputs (46) and (47):

$$\gamma_1 = v_{d,CV}^* + v_{d,AD}^* - k_{ffv} \cdot v_{d,o} + l_f \cdot \omega_{VSM} \cdot i_{q,CV} \tag{46}$$

$$\gamma_2 = v_{q,CV}^* + v_{q,AD}^* - k_{ffv} \cdot v_{q,o} - l_f \cdot \omega_{VSM} \cdot i_{d,CV} \tag{47}$$

Similarly, the voltage controller is initialized. The steady-state values of the voltage references are equal to the measured voltage $\boldsymbol{v}_o$. The state variables of the voltage PI controllers are given by (48) and (49):

$$\epsilon_1 = i_{d,CV}^* - k_{ffi} \cdot i_{d,o} + c_f \cdot \omega_{VSM} \cdot v_{q,o} \tag{48}$$

$$\epsilon_2 = i_{q,CV}^* - k_{ffi} \cdot i_{q,o} - c_f \cdot \omega_{VSM} \cdot v_{d,o} \tag{49}$$

Since the voltage reference for the voltage controller $\boldsymbol{v}_o^*$ is equal to the measured voltage $\boldsymbol{v}_o$, the voltage amplitude reference v^{**} can be expressed by (50):

$$v^{**} = v_{d,o}^* + i_{d,o} \cdot r_v - \omega_{VSM} \cdot l_v \cdot i_{q,o} \tag{50}$$

Note that in steady-state v^{**} should be equal to the $\boldsymbol{v}_{VSM}$ (39), that is, in the VSM reference frame, the q-component is zero and only the d-component persists and is analogous to the internal EMF of a synchronous generator.

The input external voltage reference of the reactive power controller in steady-state can be calculated by equation (51). But since the derivations are zero, the filtered value $\hat{q}$ correspond to the measured reactive power q. And since in steady-state, the measured reactive power is equal to the reactive power setpoint, the external voltage setpoint is equal to the desired value of the internal virtual EMF $\boldsymbol{v}_{VSM}$.

$$v^* = v^{**} - k_q(q^* - \hat{q}) = v^{**} \tag{51}$$

VI. DYNAMIC SIMULATION EXAMPLES

This section analyses the behavior of the described VSM model in both grid-connected and islanded operation. For simulation purposes, a load is connected in parallel to an external grid. Simulation examples show the response of the VSM to a step increase of active power of a load connected to the external grid bus. The step change happens at $t = 4$ s. The external grid is modeled as a voltage source behind transient reactance (classical model of a synchronous generator, with no AVR and turbine-governor). The control configuration described in sections III and IV is valid for both operation modes without any modification.

A. Operating in grid-connected mode

When an increase in load power occurs, the static generator increases its output power p_o to maintain power balance, as shown in Fig. 6(a). The VSM virtual rotor speed follows the grid frequency, and at the instance of the step change in load power, it releases energy from its virtual inertia to oppose the change in frequency followed by the primary frequency response to equalize the generation and consumption, and stabilize the frequency (Fig. 6(b)). Conversely, the external grid power temporarily decreases and returns to the same value since it exhibits a behavior of an unregulated SG. Analogous to a SG, with an increase in power demand, the virtual rotor frequency decreases. As soon as the power balance is re-established, ω_{VSM} stabilizes and remains at a quasi-steady-state value, but lower from the frequency setpoint. The VSM phase displacement will also increase as shown in Fig. 6(c).

B. Operating in islanded mode

In islanded mode, the static generator is set up as a reference machine while feeding the local load. The response of the virtual rotor frequency ω_{VSM} in islanded mode is similar to the response in grid-connected mode. However, ω_{VSM} experiences more oscillations due to the lack of physical inertia in the system, as shown in Fig. 7(b). It also requires more time to stabilize at a new value. The static generator will respond to an increase in load power in islanded mode with an instantaneous increase in output power p_o (Fig. 7(a)), provided there is enough stored energy in the buffer of the converter-interfaced source.

C. Sensitivity of the VSM model to parameter changes

In these simulations the VSM also works standalone, powering the local load at the end of the line. A step increase in load power is introduced at $t = 4$ s.

The mechanical constant T_a is equivalent to $2H$ in a traditional SM, playing a vital role in maintaining the frequency stability of the power system. The higher the value of the mechanical constant the smaller the frequency nadir, but the settling time is longer. However, lower value of T_a may cause unwanted oscillations in the system. According to Fig. 8(a), it can be deduced that T_a has no impact on the quiescent value, just like an actual machine. The virtual inertia has the same effect as the real inertia, ie. the system is more stable when
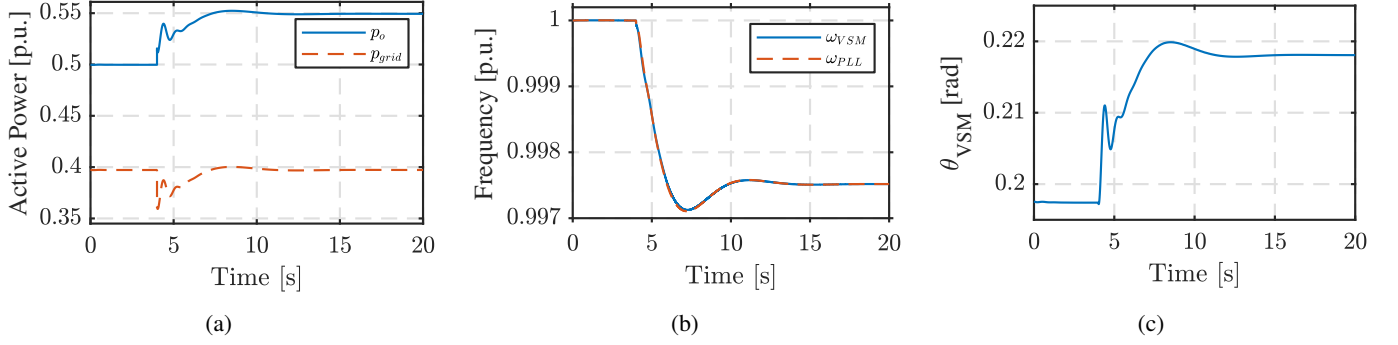
Figure 6: Results for grid-connected operation: (a) VSM output power and active power of the external grid; (b) Angular frequencies; (c) the VSM phase displacement
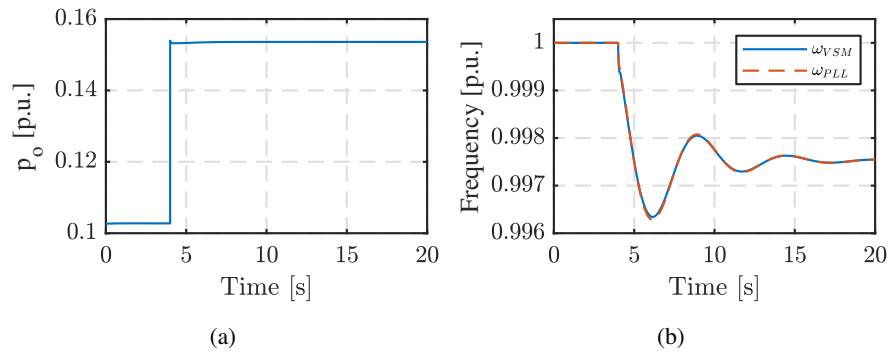

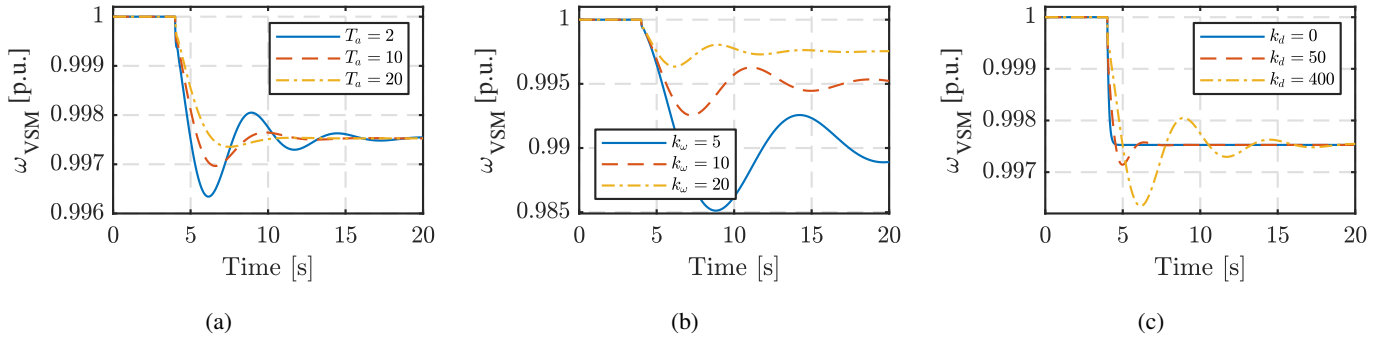Figure 7: Results for islanded operation: (a) VSM output power; (b) Angular frequencies

Figure 8: The VSM response to different values of: (a) T_a; (b) k_w; (c) k_d

it increases, provided that the converter-interfaced source has an adequate energy buffer.

With droop gain k_ω, the power-frequency droop is achieved defining the steady-state frequency deviation after a generation-load disturbance. As shown in Fig. 8(b), the lower the value of k_ω, the bigger the frequency nadir and steady-state deviation, while the settling time is longer. However, too large of a droop gain may destabilize the system.

The next parameter impacting the VSM behavior is the damping coefficient k_d. In the presented VSM implementation, the damping effect is achieved by comparing the VSM rotor frequency to the speed of the reference machine / grid

frequency which tends to drive them towards equilibrium. However, in islanded mode as well as in grid-connected mode in which the external grid is modeled as a rotating mass without primary frequency controller, this implementation, ironically, tends to destabilize the system with increasing k_d due to the PLL lag. As shown in Fig. 8(b), lower k_d value results in lower maximum deviation and settling time, while it has no impact on the quiescent value.

Alternatively, the damping term can be implemented by comparing ω_{VSM} to the nominal frequency and this would drive the VSM speed towards nominal speed. The damping term tries to emulate the stabilizing effect of damper windings

and/or rotor shaft friction and/or frequency sensitivity of load, although the latter is usually included in the load model.

VII. Conclusion

Most common virtual inertia converter control schemes: virtual synchronous machine (VSM), virtual synchronous generator (VSG) and synchronverter are often used interchangeably in the literature and may be confusing to newcomers in the field. In reality, they present three different control designs and this paper gives an overview of them and provides a clear distinction. Then, the paper shows a step-by-step tutorial procedure on how to implement a detailed dynamic VSM model in commercial power system simulation software for fundamental frequency (RMS) simulations and explains the technical and mathematical background of it. The steady-state representation of the VSM model, used to control a power converter supplied from an electric energy source, is presented. The algorithm for straightforward and modular initialization of all the variables is given which avoids solving a complex set of equations simultaneously. Finally, the paper provides a selected dynamic simulation examples to explain and show the impact of different VSM parameters on its dynamic response as well as to verify the ability of the VSM model to operate in grid-connected and islanded modes. Finally, as a contribution of the tutorial the presented models are made open access available to the research community for further upgrades and customized implementation [40].

Appendix

Table II: Parameters of the VSM simulation model

Name	Value
Nominal/base power S_b	1 MVA
Base AC voltage $V_{b,\mathrm{AC}}$ (RMS, line-to-line)	690 V
Base angular frequency ω_b	$2\pi50$
Grid resistance r_g	0.01 p.u.
Grid inductance l_g	0.2 p.u.
Filter resistance r_f	0.003 p.u.
Filter inductance l_f	0.08 p.u.
Filter capacitance c_f	0.074 p.u.
Active power reference p^*	0.5 p.u.
Virtual mechanical time constant T_a	2 s
VSM damping constant k_d	400
Frequency droop gain k_ω	20 p.u.
Reference value of VSM angular frequency ω_{VSM}^*	1 p.u.
PLL cut-off frequency ω_{LP}	500 rad/s
PLL gain: $k_{p,PLL}$, $k_{i,PLL}$	10, 30
Reactive power reference q^*	0.0 p.u.
Reactive power filter ω_f	1000 rad/s
Reactive power droop gain k_q	0.3 p.u.
Virtual resistance r_v	0.0 p.u.
Virtual inductance l_v	0.2 p.u.
Voltage controller gain: k_{pv}, k_{iv}	2, 10
Active damping filter ω_{AD}	50 rad/s
Active damping gain k_{AD}	0.5 p.u.
Current controller gain: k_{pc}, k_{ic}	0.1, 10
DC link voltage v_{DC}	1.0 p.u.

References

[1] "What is carbon neutrality and how can it be achieved by 2050?" European Parliament, 2020.

[2] I. Kucuk and T. Thangamani, "Rms modeling of grid-forming power electronics for renewable energy power plant integration and classical power system stability studies," Master's thesis, Aalborg University, 2020.

[3] A. Alfergani, A. Khalil, and Z. Rajab, "Networked control of ac microgrid," *Sustainable cities and society*, vol. 37, pp. 371–387, 2018.

[4] O. Mohammed, A. Otuoze, S. Salisu, O. Ibrahim, and N. Rufa'i, "Virtual synchronous generator: an overview," *Nigerian Journal of Technology*, vol. 38, no. 1, pp. 153–164, 2019.

[5] O. Bahwal, "Implementation of virtual synchronous machine to allow high penetration of converter connected generation," Master's thesis, Chalmers University of Technology, 2018.

[6] "Statistical review of world energy 2020," BP, 2020.

[7] P. Tielens and D. Van Hertem, "The relevance of inertia in power systems," *Renewable and Sustainable Energy Reviews*, vol. 55, pp. 999–1009, March 2016.

[8] F. Milano, F. Dörfler, G. Hug, D. J. Hill, and G. Verbič, "Foundations and challenges of low-inertia systems (invited paper)," in *2018 Power Systems Computation Conference (PSCC)*, June 2018, pp. 1–25, doi: 10.23919/PSCC.2018.8450880.

[9] A. Ulbig, T. S. Borsche, and G. Andersson, "Analyzing Rotational Inertia, Grid Topology and their Role for Power System Stability," *IFAC-PapersOnLine*, vol. 48, no. 30, pp. 541–547, 2015.

[10] B. K. Poolla, D. Groß, and F. Dörfler, "Placement and implementation of grid-forming and grid-following virtual inertia and fast frequency response," *IEEE Transactions on Power Systems*, vol. 34, no. 4, pp. 3035–3046, 2019.

[11] A. Ademola-Idowu and B. Zhang, "Optimal design of virtual inertia and damping coefficients for virtual synchronous machines," in *2018 IEEE Power & Energy Society General Meeting (PESGM)*. IEEE, 2018, pp. 1–5.

[12] U. Markovic, O. Stanojev, P. Aristidou, E. Vrettos, D. S. Callaway, and G. Hug, "Understanding small-signal stability of low-inertia systems," *IEEE Transactions on Power Systems*, 2021, early access.

[13] "Requirements for Generators," https://www.entsoe.eu/network_codes/rfg/, 2016, COMMISSION REGULATION (EU) 2016/631 of 14 April 2016 establishing a network code on requirements for grid connection of generators.

[14] "Innovative solutions for 100% renewable power in sweden," International Renewable Energy Agency, Tech. Rep., 2020.

[15] M. Nedd, J. Browell, A. Egea-Alvarez, K. Bell, R. Hamilton, S. Wang, and S. Brush, "Operating a zero carbon gb power system in 2025: Frequency and fault current [annexes-review of system and network issues, frequency stability, power electronic devices and fault current, & market needs]," University of Strathclyde, Tech. Rep., 2020.

[16] "Dynamic containment," National Grid ESO, 2020. [Online]. Available: https://www.nationalgrideso.com/document/165141/download

[17] Z. H. Rather, Z. Chen, and P. Thøgersen, "Challenges of danish power system and their possible solutions," in *2012 IEEE International Conference on Power System Technology (POWERCON)*. IEEE, 2012, pp. 1–6.

[18] J. R. Pillai and B. Bak-Jensen, "Integration of vehicle-to-grid in the western danish power system," *IEEE transactions on sustainable energy*, vol. 2, no. 1, pp. 12–19, 2010.

[19] J. Rocabert, A. Luna, F. Blaabjerg, and P. Rodriguez, "Control of power converters in ac microgrids," *IEEE transactions on power electronics*, vol. 27, no. 11, pp. 4734–4749, 2012.

[20] R. Heydari, M. Savaghebi, and F. Blaabjerg, "Fast frequency control of low-inertia hybrid grid utilizing extended virtual synchronous machine," in *2020 11th Power Electronics, Drive Systems, and Technologies Conference (PEDSTC)*. IEEE, 2020, pp. 1–5.

[21] A. Tayyebi, D. Groß, A. Anta, F. Kupzog, and F. Dörfler, "Interactions of grid-forming power converters and synchronous machines," *arXiv preprint arXiv:1902.10750*, 2019.

[22] B. Weise, A. Korai, and A. Konstantin, "Comparison of selected grid-forming converter control strategies for use in power electronic dominated power systems," in *18th Wind Integration Workshop*, 2019, pp. 1–9.

[23] K. Y. Yap, C. R. Sarimuthu, and J. M.-Y. Lim, "Virtual inertia-based inverters for mitigating frequency instability in grid-connected renewable energy system: A review," *Applied Sciences*, vol. 9, no. 24, p. 5300, 2019.

[24] Z. Lv and Q.-C. Zhong, "Control of modular multilevel converters as virtual synchronous machines," in *2017 IEEE Power & Energy Society General Meeting*. IEEE, 2017, pp. 1–5.

[25] S. D'Arco and J. A. Suul, "Virtual synchronous machines—classification of implementations and analysis of equivalence to droop controllers for microgrids," in *2013 IEEE Grenoble Conference*. IEEE, 2013, pp. 1–7.

[26] S. D'Arco, J. A. Suul, and O. B. Fosso, "A virtual synchronous machine implementation for distributed control of power converters in smartgrids," *Electric Power Systems Research*, vol. 122, pp. 180 – 197, 2015. [Online]. Available: http://www.sciencedirect.com/science/article/pii/S0378779615000024

[27] S. D'Arco, J. A. Suul, and O. B. Fosso, "Small-signal modelling and parametric sensitivity of a virtual synchronous machine," in *2014 Power Systems Computation Conference*. IEEE, 2014, pp. 1–9.

[28] H.-P. Beck and R. Hesse, "Virtual synchronous machine," in *2007 9th International Conference on Electrical Power Quality and Utilisation*. IEEE, 2007, pp. 1–6.

[29] Y. Chen, R. Hesse, D. Turschner, and H.-P. Beck, "Dynamic properties of the virtual synchronous machine (visma)," *Proc. ICREPQ*, vol. 11, 2011.

[30] U. Tamrakar, D. Shrestha, M. Maharjan, B. P. Bhattarai, T. M. Hansen, and R. Tonkoski, "Virtual inertia: Current trends and future directions," *Applied Sciences*, vol. 7, no. 7, p. 654, 2017.

[31] M. Yu, A. J. Roscoe, C. D. Booth, A. Dysko, R. Ierna, J. Zhu, and H. Urdal, "Use of an inertia-less virtual synchronous machine within future power networks with high penetrations of converters," in *2016 Power Systems Computation Conference (PSCC)*. IEEE, 2016, pp. 1–7.

[32] A. J. Roscoe, M. Yu, R. Ierna, J. Zhu, A. Dyśko, H. Urdal, and C. Booth, "A vsm (virtual synchronous machine) convertor control model suitable for rms studies for resolving system operator/owner challenges," in *15th Wind Integration Workshop*, 2016.

[33] L. A. Lopes *et al.*, "Self-tuning virtual synchronous machine: A control strategy for energy storage systems to support dynamic frequency control," *IEEE Transactions on Energy Conversion*, vol. 29, no. 4, pp. 833–840, 2014.

[34] M. Yu, A. Dyśko, A. Roscoe, C. Booth, R. Ierna, H. Urdal, and J. Zhu, "Effects of swing equation-based inertial response (sebir) control on penetration limits of non-synchronous generation in the gb power system," in *International Conference on Renewable Power Generation (RPG 2015)*, 2015, pp. 1–6.

[35] J. Driesen and K. Visscher, "Virtual synchronous generators," in *2008 IEEE Power and Energy Society General Meeting - Conversion and Delivery of Electrical Energy in the 21st Century*, 2008, pp. 1–3.

[36] Q.-C. Zhong and G. Weiss, "Synchronverters: Inverters that mimic synchronous generators," *IEEE transactions on industrial electronics*, vol. 58, no. 4, pp. 1259–1267, 2010.

[37] F. S. Rahman, T. Kerdphol, M. Watanabe, and Y. Mitani, "Optimization of virtual inertia considering system frequency protection scheme," *Electric Power Systems Research*, vol. 170, pp. 294–302, 2019.

[38] M. Van Wesenbeeck, S. De Haan, P. Varela, and K. Visscher, "Grid tied converter with virtual kinetic storage," in *2009 IEEE Bucharest PowerTech*. IEEE, 2009, pp. 1–7.

[39] H. Bevrani, T. Ise, and Y. Miura, "Virtual synchronous generators: A survey and new perspectives," *International Journal of Electrical Power & Energy Systems*, vol. 54, pp. 244–254, jan 2014. [Online]. Available: https://www.sciencedirect.com/science/article/pii/S0142061513003062

[40] "Virtual Synchronous Machine model for RMS simulations in DIgSILENT PowerFactory," https://applygit.zvne.fer.hr/mkrpan/vsm-rms-model-powerfactory, 2021.